Noname manuscript No.
(will be inserted by the editor)

Final Report: Mach-Zehnder and Michelson Interferometers

Mason Bressler

the date of receipt and acceptance should be inserted later

Abstract This report describes the design and fabrication of Mach-Zehnder interferometers (MZI) and Michelson Interferometers. Variations on the designs include path length differences to observe how the free spectral range (FSR) is impacted.

1 Introduction

The Mach-Zehnder interferometer is a device used to measure phase shift between two beams of light. A single source input is split between two branches and then recombined. In a Michelson interferometer, only a single beam splitter is used and the light takes two passes before recombining.

2 Theory

An imbalanced MZI consists of a single input split into two branches of unequal length (ΔL) then recombined to a single output. In the Y-branch splitter the incident electric field, E_i , and corresponding intensity, I_i , are equally split into the two branches with electric field outputs of $E_1 = E_2 = \frac{E_i}{\sqrt{2}}$ and intensity $I_1 = I_2 = \frac{I_i}{2}$. For the Y-branch combiner the same equations apply and with two inputs the output field is a vector summation divided by $\sqrt{2}$. For plane wave light propagation, $E = E_o e^{i(\omega t - \beta z)}$, and the propagation constant of light, $\beta = \frac{2\pi n}{\lambda}$, where n is the index of refraction. The light split into each arm observe different path lengths, L_1 and L_2, and therefore the expressions for electric fields at the end of each waveguide, in the lossless case, are:

$$E_{o1} = E_1 e^{-i\beta_1 L_1} = \frac{E_i}{\sqrt{2}} e^{-i\beta_1 L_1}$$

$$E_{o2} = E_2 e^{-i\beta_2 L_2} = \frac{E_i}{\sqrt{2}} e^{-i\beta_2 L_2}$$

The combined light is therefore:

$$E_o = \frac{1}{\sqrt{2}}(E_{o1} + E_{o2}) = \frac{E_i}{2}(e^{-i\beta_1 L_1} + e^{-i\beta_2 L_2})$$

Therefore the intensity is:

$$I_o = \frac{I_i}{4}\left|e^{-i\beta_1 L_1} + e^{-i\beta_2 L_2}\right|^2 = \frac{I_i}{4}\left[2\cos\left(\frac{\beta_1 L_1 - \beta_2 L_2}{2}\right)\right]^2$$

$$= I_i \cos^2\left(\frac{\beta_1 L_1 - \beta_2 L_2}{2}\right) = \frac{I_i}{2}\left[1 + \cos\left(\beta_1 L_1 - \beta_2 L_2\right)\right]$$

For an imbalanced interferometer the waveguides are the same and hence $\beta_1 = \beta_2$ however the lengths are different, therefore $\Delta L = L_1 - L_2$

And the transfer function of the full MZI is:

$$\frac{I_o}{I_i} = \frac{1}{2}\left[1 + \cos\left(\beta \Delta L\right)\right]$$

3 Modelling and Simulation

There are nine total designs submitted for this fabrication run. All designs, with the exception of two, utilize a waveguide with $500nm$ width and $220nm$ height and are TE mode. Two layouts use $450nm$ width and $220nm$ height to compare TE and TM modes of operation.

Mason Bressler
Affiliation not available

3.0.1

3.1 *A. Waveguide*

The simulated mode profiles for the $500nm$ waveguide are presented below: Fig. 1 shows the effective index, Fig. 2 is the group index, and Fig. 3 is the TE mode Electric field intensity.

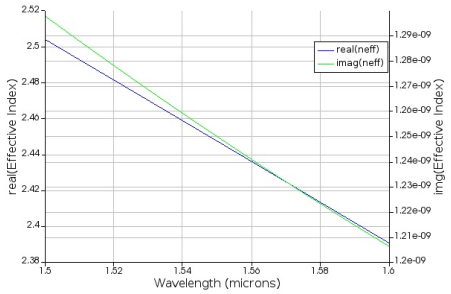

Fig. 1 Real and imaginary components of effective index of the waveguide versus wavelength: TE mode 1

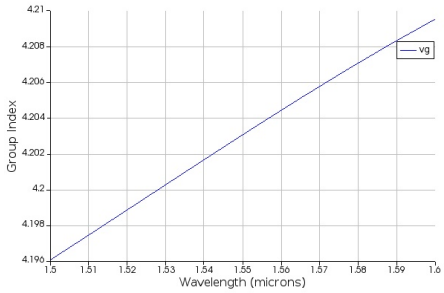

Fig. 2 Group index of the waveguide versus wavelength: TE mode 1

The simulated mode profiles for the $450nm$ waveguide are presented below: Fig. 4 shows the effective index, Fig. 5 is the group index, and Fig. 6 is the TE mode Electric field intensity. Figures 7 - 9 show the same plots for the TM mode 1 profile.

The free spectral range (FSR) is the distance between adjacent peaks in the transferfunction.For a MZI the FSR is shown to be:

$$FSR\ [m]\ =\ \frac{\lambda^2}{n_g \Delta L}$$

The Michelson interferometer has two passes so the FSR is below:

$$FSR\ [m]\ =\ \frac{\lambda^2}{2n_g \Delta L}$$

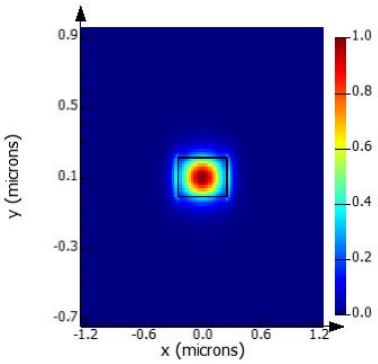

Fig. 3 TE mode 1 electric field intensity profile in waveguide

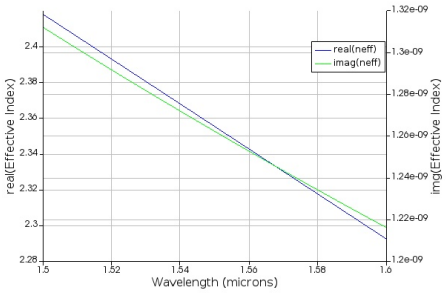

Fig. 4 Real and imaginary components of effective index of the waveguide versus wavelength: TE mode 1

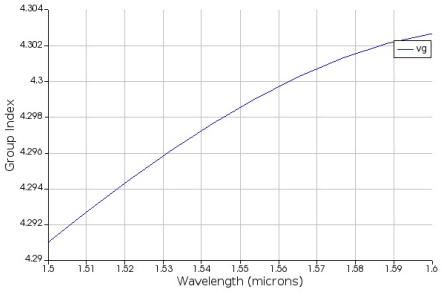

Fig. 5 Group index of the waveguide versus wavelength: TE mode 1

The FSR for the different ΔL values and interferometer types for all designs submitted for fabrication is shown below in table 1.

Finally a simulation was completed of the baseline conditions: MZI with $\Delta L = 100\mu m$ in TE mode 1 using Lumerical Interconnect to obtain the transfer function. Fibre grating couplers are included in the simulation.

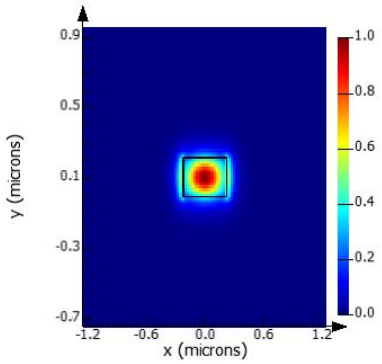

Fig. 6 TE mode 1 electric field intensity profile in waveguide

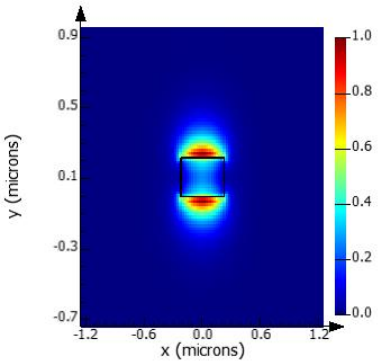

Fig. 9 TM mode 1 electric field intensity profile in waveguide

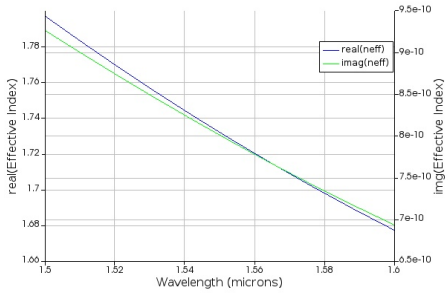

Fig. 7 7Real and imaginary components of effective index of the waveguide versus wavelength: TM mode 1

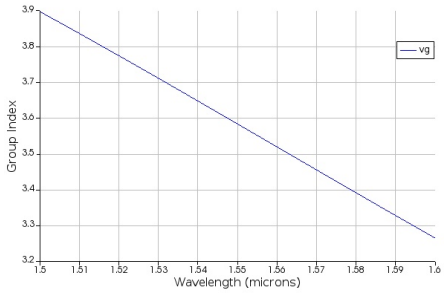

Fig. 8 Group index of the waveguide versus wavelength: TM mode 1

Type	Mode	ΔL (um)	FSR (nm)	ng	Lambda (nm)
MZI	TE	50	11.18	4.3	1550
MZI	TM	50	13.41	3.58	1550
MZI	TE	100	5.72	4.2	1550
MZI	TE	200	2.86	4.2	1550
MZI	TE	300	1.91	4.2	1550
Michelson	TE	100	2.86	4.2	1550
Michelson	TE	200	1.43	4.2	1550

Table 1 FSR calculations for different lengths and interferometer types

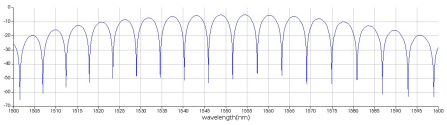

Fig. 10 MZI simulation using Lumerical Interconnect with path length difference of 100um

4 Fabrication

Chips were fabricated at two foundries: Applied Nanotools and Washington Nanofabrication Facility. The following are the process descriptions.

4.1 Washington Nanofabrication Facility (WNF) silicon photonics process:

The devices were fabricated using 100 keV Electron Beam Lithography [1]. The fabrication used silicon-on-insulator wafer with 220 nm thick silicon on 3 μm thick silicon dioxide. The substrates were 25 mm squares diced from 150 mm wafers. After a solvent rinse and hot-plate dehydration bake, hydrogen silsesquioxane resist (HSQ, Dow-Corning XP-1541-006) was spin-coated at 4000 rpm, then hotplate baked at 80 °C for 4 minutes. Electron beam lithography was performed using a JEOL JBX-6300FS system operated at 100 keV energy, 8 nA beam current, and 500 μm exposure field size. The machine grid used for shape placement was 1 nm, while the beam stepping grid, the spacing between dwell points during the shape writing, was 6 nm. An exposure dose of 2800 μC/cm2 was used. The resist was developed by immersion in 25% tetramethylammonium hydroxide for 4 minutes, followed by a flowing deionized water rinse for 60 s, an isopropanol rinse for 10 s, and then blown dry with nitrogen. The silicon was removed from unexposed areas using inductively cou-

pled plasma etching in an Oxford Plasmalab System 100, with a chlorine gas flow of 20 sccm, pressure of 12 mT, ICP power of 800 W, bias power of 40 W, and a platen temperature of 20 °C, resulting in a bias voltage of 185 V. During etching, chips were mounted on a 100 mm silicon carrier wafer using perfluoropolyether vacuum oil. Cladding oxide was deposited using plasma enhanced chemical vapor deposition (PECVD) in an Oxford Plasmalab System 100 with a silane (SiH4) flow of 13.0 sccm, nitrous oxide (N2O) flow of 1000.0 sccm, high-purity nitrogen (N2) flow of 500.0 sccm, pressure at 1400mT, high-frequency RF power of 120W, and a platen temperature of 350C. During deposition, chips rest directly on a silicon carrier wafer and are buffered by silicon pieces on all sides to aid uniformity.

4.2 Applied Nanotools, Inc. NanoSOI process:

The photonic devices were fabricated using the NanoSOI MPW fabrication process by Applied Nanotools Inc. (http://www.appliednt.com/nanosoi; Edmonton, Canada) which is based on direct-write 100 keV electron beam lithography technology. Silicon-on-insulator wafers of 200 mm diameter, 220 nm device thickness and 2 µm buffer oxide thickness are used as the base material for the fabrication. The wafer was pre-diced into square substrates with dimensions of 25x25 mm, and lines were scribed into the substrate backsides to facilitate easy separation into smaller chips once fabrication was complete. After an initial wafer clean using piranha solution (3:1 H2SO4:H2O2) for 15 minutes and water/IPA rinse, hydrogen silsesquioxane (HSQ) resist was spin-coated onto the substrate and heated to evaporate the solvent. The photonic devices were patterned using a Raith EBPG 5000+ electron beam instrument using a raster step size of 5 nm. The exposure dosage of the design was corrected for proximity effects that result from the backscatter of electrons from exposure of nearby features. Shape writing order was optimized for efficient patterning and minimal beam drift. After the e-beam exposure and subsequent development with a tetramethylammonium sulfate (TMAH) solution, the devices were inspected optically for residues and/or defects. The chips were then mounted on a 4" handle wafer and underwent an anisotropic ICP-RIE etch process using chlorine after qualification of the etch rate. The resist was removed from the surface of the devices using a 10:1 buffer oxide wet etch, and the devices were inspected using a scanning electron microscope (SEM) to verify patterning and etch quality. A 2.2 µm oxide cladding was deposited using a plasma-enhanced chemical vapour deposition (PECVD) process based on tetraethyl orthosilicate (TEOS) at 300ºC. Reflectrometry measurements were performed throughout the process to verify the device layer, buffer oxide and cladding thicknesses before delivery.

5 Experimental Data

To characterize the devices, a custom-built automated test setup [2, 6] with automated control software written in Python was used [3]. An Agilent 81600B tunable laser was used as the input source and Agilent 81635A optical power sensors as the output detectors. The wavelength was swept from 1500 to 1600 nm in 10 pm steps. A polarization maintaining (PM) fibre was used to maintain the polarization state of the light, to couple the TE polarization into the grating couplers [4]. A 90º rotation was used to inject light into the TM grating couplers [4]. A polarization maintaining fibre array was used to couple light in/out of the chip [5].

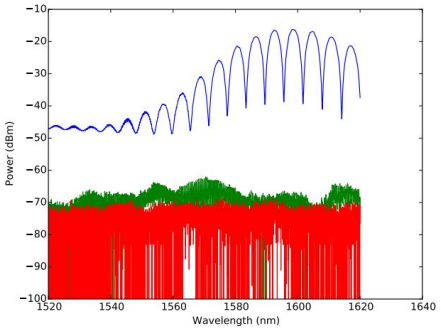

Fig. 11 Measured transmission spectrum on a Mach-Zehnder Interferometer with a path length difference of 100 microns.

6 Analysis

Monte Carlo simulations were performed using KLayout and Lumerical Interconnect to better predict measured performance over process variation. Simulations were performed using typical process variations for Applied Nanotool's process and 50 die sites per wafer over a single wafer. The results are shown below for the MZI with $\Delta L = 100\mu m$: MZI transmission spectrum in Fig. 12 and MZI FSR histogram in Fig. 13

The raw measured data was processed using Python scripts and corrected to remove the effects of the fibre grating couplers and is shown below. Fig. 14 shows the MZI

The data processing in Python is also able to extract the FSR and ground index for the measured data.

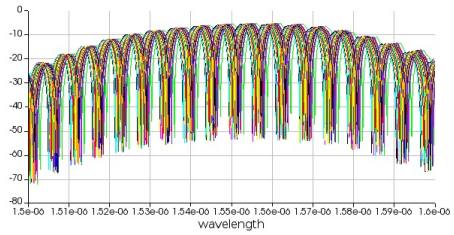

Fig. 12 MZI transmission spectrum Monte Carlo simulation: $\Delta L = 100\mu m$

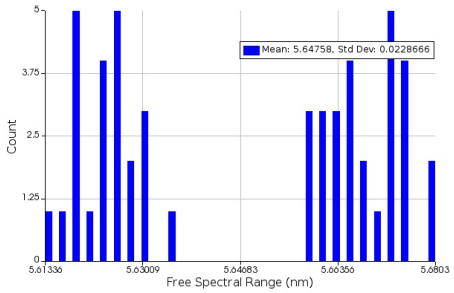

Fig. 13 Free Spectral Range Histogram: $\Delta L = 100\mu m$

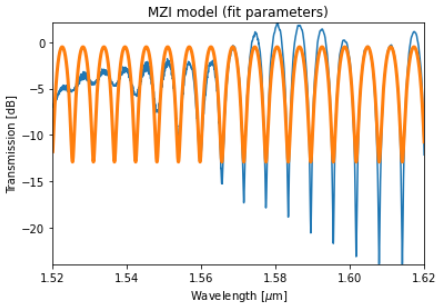

Fig. 14 Measured MZI corrected data: $\Delta L = 100\mu m$

The FSR was extracted from the measured data and shown to be 6.05nm which is then compared to the equation based calculations shown in Table 1, for an MZI with $\Delta L = 100\mu m$ the FSR is 5.72nm. These values show very close agreement. Using the measured data the group index was also extracted and is shown in Fig. 15 below. Similarly, the group index extracted value of 4.16 is also very close to the calculated value of 4.2 in Table 1.

7 Conclusion

A Mach-Zehnder interferometer with path length difference of 100um at 1550nm was designed using Lumerical Mode and Interconnect software, layout created using KLayout and then fabricated at Applied Nanotools

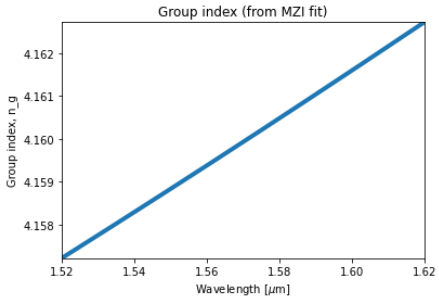

Fig. 15 MZI with $\Delta L = 100\mu m$: extracted group index

in Edmonton Canada. Measured data was processed and key parameters extracted such as the group index and free spectral range which were shown to have close agreement to the expected performance obtained in simulations.

8 Acknowledgements

I acknowledge the edX UBCx Phot1x Silicon Photonics Design, Fabrication and Data Analysis course, which is supported by the Natural Sciences and Engineering Research Council of Canada (NSERC) Silicon Electronic-Photonic Integrated Circuits (SiEPIC) Program. The devices were fabricated by Richard Bojko at the University of Washington Washington Nanofabrication Facility, part of the National Science Foundation's National Nanotechnology Infrastructure Network (NNIN), and Cameron Horvath at Applied Nanotools, Inc. Hossam Shoman performed the measurements at The University of British Columbia. We acknowledge Lumerical Solutions, Inc., Mathworks, Mentor Graphics, Python, and KLayout for the design software.

9 References

[1] R. J. Bojko, J. Li, L. He, T. Baehr-Jones, M. Hochberg, and Y. Aida, "Electron beam lithography writing strategies for low loss, high confinement silicon optical waveguides," J. Vacuum Sci. Technol. B 29, 06F309 (2011)

[2] Lukas Chrostowski, Michael Hochberg, chapter 12 in "Silicon Photonics Design: From Devices to Systems", Cambridge University Press, 2015

[3] http://siepic.ubc.ca/probestation, using Python code developed by Michael Caverley.

[4] Yun Wang, Xu Wang, Jonas Flueckiger, Han Yun, Wei Shi, Richard Bojko, Nicolas A. F. Jaeger, Lukas Chrostowski, "Focusing sub-wavelength grating couplers with low back reflections for rapid prototyping of silicon photonic circuits", Optics Express Vol. 22, Issue 17, pp. 20652-20662 (2014) doi: 10.1364/OE.22.020652